buildings

MDPI

Article

Impact of Steel Fiber Volume Fraction and Morphology on the Strength of Recycled Aggregate Concrete

Peibo You [1], Zhili Ma [2], Lijuan Zhang [3], Yi Wang [1], Qi Feng [4,*] and Li Li [2,*]

[1] Department of Civil and Transportation Engineering, Henan University of Urban Construction, Pingdingshan 467036, China; 30070513@huuc.edu.cn (P.Y.); 30010615@huuc.edu.cn (Y.W.)
[2] College of Water Resources and Architectural Engineering, Northwest A&F University, Yangling 712100, China; 13399098560@nwafu.edu.cn
[3] School of Mechanics and Safety Engineering, Zhengzhou University, Zhengzhou 450001, China; zhanglj0526@zzu.edu.cn
[4] Guangxi Key Lab of Road Structure and Materials, Nanning 530007, China
* Correspondence: 32186008@mail.dlut.edu.cn (Q.F.); drlili@nwafu.edu.cn (L.L.)

Abstract: Steel-fiber-reinforced recycled coarse aggregate concrete (SFRCAC) has great potential for use in structural members due to environmental and economic reasons. A comparison of SF's reinforcing effect on the strength of RCAC with natural recycled coarse aggregate concrete (NCAC) was conducted through experiments and analysis. Three types of steel fiber—milling (MF), shear-wave (SWF), and both-end hooked (BF)—were used. The SF volume fraction (V_f) was taken as 0, 0.5%, 1.0%, 1.5%, and 2%. The results show that SF has a similar reinforcing effect on NCAC and RCAC. The reinforcing effect of SF on the strength of RCAC is relevant to the strength of the RCAC matrix. The suitable content range of SF is from 0.5% to 1.5% in terms of the reinforcement effects on the compressive strength (f_{fcu}) and splitting tensile strength (f_{fts}) of RCAC. SF with a higher aspect ratio (AR) has a better reinforcing effect on the splitting tensile strength (f_{fts}) and flexural strength (f_{ftm}) of RCAC. The equations of f_{fts}/f_{ts} and f_{ftm}/f_{tm} with the characteristic parameters of steel fiber (λ_f) were put forward to accurately determine the dosage of SF.

Keywords: recycled coarse aggregate concrete; steel fiber; reinforcing effect; dosage determination

check for updates

Citation: You, P.; Ma, Z.; Zhang, L.; Wang, Y.; Feng, Q.; Li, L. Impact of Steel Fiber Volume Fraction and Morphology on the Strength of Recycled Aggregate Concrete. *Buildings* **2023**, *13*, 2341. https://doi.org/10.3390/buildings13092341

Academic Editors: Flavio Stochino and Bo-Tao Huang

Received: 4 July 2023
Revised: 5 September 2023
Accepted: 11 September 2023
Published: 15 September 2023

Copyright: © 2023 by the authors. Licensee MDPI, Basel, Switzerland. This article is an open access article distributed under the terms and conditions of the Creative Commons Attribution (CC BY) license (https://creativecommons.org/licenses/by/4.0/).

1. Introduction

Concrete is the most widely utilized building material in the construction industry and is a great consumer of natural resources. Making up waste concrete into recycled coarse aggregate (RCA) to produce new concrete can reduce the impact of the construction industry on the environment [1–5]. RCA is mainly made of natural coarse aggregate (NCA) and the clung cement mortar, in which the clung cement mortar on RCA has higher porosity, higher water absorption, and lower strength than that on NCA [6]. Compared with NCA, RCA has much higher water absorption [7] and lower apparent density [8]. Additionally, a large number of microcracks are produced in the process of crushing waste concrete, which causes a higher crushing index and reduces the soundness property of RCA [9]. Replacing NCA with RCA decreases the durability and strength of recycled coarse aggregate concrete (RCAC) and increases its shrinkage strain [10–12]. Because of its poor properties, the application of RCAC is limited. In China, RCAC is only feasible as backfill and subgrade material, or for self-bearing members in civil engineering [13,14].

The addition of double hooked-end steel fiber (SF) to RCAC at a fiber volume content of 1% led to an increase of 60% in the splitting tensile strength (f_{fts}) and 88% in the flexural strength (f_{ftm}) at 28 days [15]. The addition of SF improves the mechanical properties of the RCAC; in particular, it better controls its fracture process [16]. It has been well confirmed that the incorporation of SF improves the working performance of RCAC, including better crack resistance, ductility, and toughness [17–19]. Also, the combination of SF and RCA

has great environmental and economic positive effects; SF can prevent the development of cracks in concrete through the bridging of the fibers and improve the strength and toughness of concrete [18,20,21]. SF-reinforced RCAC has great application potential for structural members [22].

However, the reinforcing effect of SF type and content on the strength of RCAC is still unclear, and there is no proper calculation method for the dosage determination of steel fiber in the mixture proportion design of SF-reinforced RCAC, which is dependent only on the experience of designer. The dosage of SF determined by experience is generally larger than that for actual demand, leading to waste of SF material. Therefore, the reinforcing effect of SF type and content on the strength of RCAC was studied by experiments for this paper, and the dosage determination method was put forward based on experimental research and analysis of the results. The list of abbreviations is shown in Table 1.

Table 1. List of abbreviations.

Name	Abridge
Steel-fiber-reinforced recycled coarse aggregate concrete	SFRCAC
Natural recycled coarse aggregate concrete	NCAC
Steel fibers	SF
Milling fiber	MF
Shear-wave fiber	SWF
Both-end hooked fiber	BF
Volume fraction	V_f
Compressive strength	f_{fcu}
Splitting tensile strength	f_{fts}
Flexural strength	f_{ftm}

2. Experimental Program

2.1. Materials

General Portland cement (P.O 42.5) conforming to the stipulations in GB 175 [23] was used in all mixtures; the properties of the cement are shown in Table 2. The coarse aggregate included NCA and RCA. The NCA was crushed limestone with continuous grading of particle sizes from 4.75 mm to 20 mm. The RCA was obtained from waste concrete specimens with compressive strength (f_{fcu}) ranging from 30 MPa to 50 MPa, and of unknown age. The waste concrete was collected and crushed through a jaw crusher, and then screened through sieves with a maximum size of 20 mm and a minimum size of 4.75 mm. The grading of the NCA and RCA was within the upper and lower limit bounds of ASTMC33/C33M-13 [24]. The fine aggregate was river sand with a fineness modulus of 2.67. The physical properties of all aggregates used in the test, obtained using the test methods in Chinese standards GB/T 25177 [25] and GB/T 14685 [26], are shown in Table 3. The NCA used was in the oven-dried condition. The particle size distributions of the coarse aggregates are shown in Figure 1. It can be inferred from Table 3 that the RCA, compared with the NCA, had the higher water absorption, void ratio, and crushing index, but lower apparent density. To remedy the adverse effects of RCA on the working performance of RCAC, it needs to be pre-wet and in the saturated surface-dry state when batching. Three types of SF, including milling (MF), shear-wave (SWF), and both-end hooked (BF), were used. Table 4 provides an overview of the characteristic parameters of the SFs.

Table 2. Physical and mechanical properties of cement.

Type	Specific Gravity (kg/m^3)	Surface Area (m^2/kg)	Standard Consistency (%)	Stability	Setting Time (Min)		Compressive Strength (MPa)		Flexural Strength (MPa)	
					Initial	Final	3 d	28 d	3 d	28 d
P.O 42.5	3100	352	24.7	Eligibility	175	220	23.5	45	5.6	8.5

Table 3. Physical properties of the coarse and fine aggregates.

Aggregate Type	Apparent Density (kg/m^3)	Loose Packing Density (kg/m^3)	Dry-Rodded Density (kg/m^3)	Water Absorption (wt%)	Crushing Index (%)	Void Ratio (%)
RCA	2640	1302	1412	4.85	17.7	50.3
NCA	2814	1568	1630	1.40	8.8	44.3
Sand	2556	1611	1486	0.56	-	-

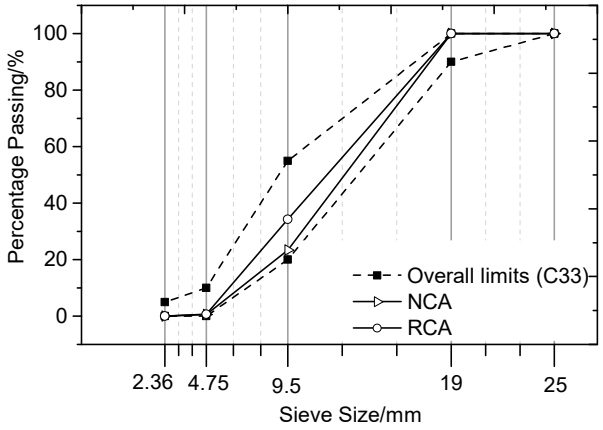


Figure 1. Size distribution curves of RCA and NCA.

Table 4. Characteristic parameters of steel fibers.

Type	Mean Length (l_f)/mm	Mean Diameter (d_f)/mm	Aspect Ratio (l_f/d_f)
Milling (MF)	32.3	0.944	34.2
Shear-wave (SWF)	30.0	0.756	39.7
Both-end hooked (BF)	62.0	0.753	82.3

2.2. Mix Proportion

All of the mixing procedures and the mixture proportions were in accordance with the Chinese regulation "Technical specification for application of fiber reinforced concrete" (JGJ/T 221-2010, 2010) [27]. The water–cement ratio was considered to be 0.48. NCA and RCA were used as coarse aggregates. The SF volume fraction (V_f) of MF was taken as 0, 0.5%, 1.0%, 1.5%, and 2%, and only 1% for SWF and BF to compare with MF. To ensure the workability of SFRCAC, for each 0.5% increase in V_f, the water content was increased by 8 kg/m^3 and the sand ratio by 3% [28]. To accurately determine the reinforcement effect of SF, one mixture for normal concrete without SF, which each group of SFRCAC corresponding to the same proportion of V_f, was also prepared. The 22 groups of mixture proportions designed are listed in Table 5.

Table 5. Mixture proportions (kg/m^3), compressive strength, splitting tensile strength, and flexural strength of SFRCAC.

Specimen No.	Water	Cement	Sand	NCA	RCA	Steel Fiber	f_{cu}/MPa	f_{ts}/MPa	f_{tm}/MPa
NC	164	342	721	1283	0	0	42.10	3.77	5.90
RC	164	342	721	0	1283	0	40.78	3.11	4.46
NCMF0.5	172	358	749	1171	0	39	42.76	3.81	6.67
NCNF0.5-C	172	358	749	1171	0	0	42.32	3.69	5.71
RCMF0.5	172	358	749	0	1171	39	42.09	3.28	5.00
RCNF0.5-C	172	358	749	0	1171	0	41.80	3.22	4.79
NCMF1.0	180	375	796	1099	0	78	48.87	5.06	7.28

Table 5. *Cont.*

Specimen No.	Water	Cement	Sand	NCA	RCA	Steel Fiber	f_{cu}/MPa	f_{ts}/MPa	f_{tm}/MPa
NCBF1.0	180	375	796	1099	0	78	45.44	5.61	16.25
NCSWF1.0	180	375	796	1099	0	78	45.37	5.19	8.13
NCNF1.0-C	180	375	796	1099	0	0	47.05	3.81	5.78
RCMF1.0	180	375	796	0	1099	78	45.56	4.12	5.74
RCBF1.0	180	375	796	0	1099	78	42.63	4.61	14.07
RCSWF1.0	180	375	796	0	1099	78	41.60	4.24	6.43
RCNF1.0-C	180	375	796	0	1099	0	38.59	3.22	4.79
NCMF1.5	188	392	842	1029	0	117	52.56	5.43	8.76
NCNF1.5-C	188	392	842	1029	0	0	49.42	3.94	6.59
RCMF1.5	188	392	842	0	1029	117	49.79	5.57	7.36
RCNF1.5-C	188	392	842	0	1029	0	45.12	3.71	5.53
NCMF2.0	196	408	886	960	0	156	52.11	5.67	9.27
NCNF2.0-C	196	408	886	960	0	0	48.29	3.23	5.65
RCMF 2.0	196	408	886	0	960	156	50.77	5.58	8.54
RCNF2.0-C	196	408	886	0	960	0	48.07	3.32	5.34

Note: RCMF1.0 indicates that the coarse aggregate is RCA, milling steel fiber, and V_f of 1.0%; RCNF1.0-C is the plain concrete with the same mix proportion as RCF1.0.

2.3. Test Specimens

Cubic specimens with a side length of 150 mm were cast for the compressive strength (f_{fcu}) and splitting tensile strength (f_{fts}) tests, while prism specimens of 100 mm × 100 mm × 400 mm were cast for the flexural strength (f_{ftm}) tests. Three identical specimens in each condition were prepared for each test.

The mixing process of SFRCAC consists of three steps: Firstly, all aggregates and SF were put into a small blender to mix for about 2 min in order to assure that the SF could be evenly distributed in the aggregates. Secondly, we added cement and continued to mix for 1 min. Finally, half of the water was added to the blender and mixed for 1 min, before adding the remaining water and mixing again for 1 min.

The fresh SFRCAC was put rapidly into molds that were pre-brushed with oil. The specimens were vibrated for 20 s. After curing in air for 24 h, the specimens were demolded carefully and placed in a curing room at approximately 95% RH and 20 °C.

2.4. Test Methods

The technology roadmap is shown in Figure 2. All of the tests were carried out after 28 days of curing. The compressive and splitting tensile strength tests were performed according to the stipulations in GB/T50081 [29] on a servohydraulic closed-loop testing machine with capacity of 3000 kN, at loading rates of 0.6 MPa/s and 0.06 MPa/s, respectively. The instrument setup used for the compressive strength test and the splitting tensile strength test is shown in Figures 3 and 4, respectively. The specimen should be put in the central position of the testing machine. The casting face of the specimen cannot be used as the splitting surface, so as to eliminate the effect of the rough casting face. One cushion block and one wood filler strip were placed between specimen and the top and bottom pressure plates, respectively. The section of cushion block was a circle with a radius of 75 mm and thickness of 20 mm. The section of filler strip was 20 mm × 4 mm. The cushion block and wood filler strip should be aligned with the centerline of the top and bottom surfaces of the specimen, respectively. The f_{fts} of the specimens was calculated as follows:

$$f_{fts} = 0.637\frac{F}{A} \quad (1)$$

where f_{fts} is the splitting tensile strength (MPa), F is the maximum applied load shown by the testing machine (N), and A is the area of the splitting surface (mm^2).

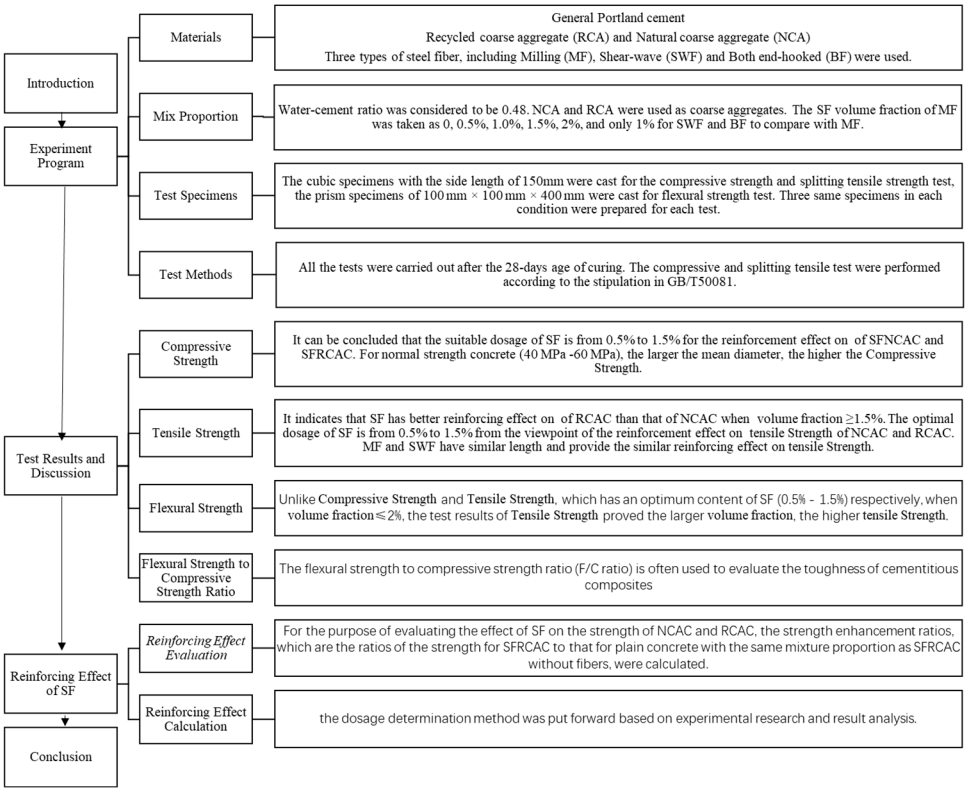


Figure 2. Technology roadmap.

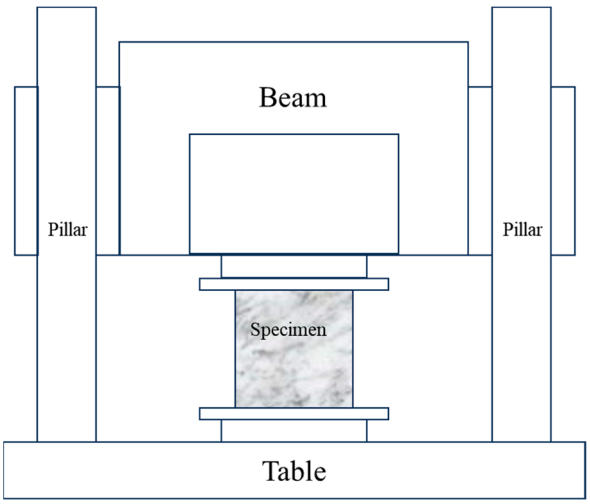


Figure 3. Instrument setup for the compressive strength tests.

The flexural tests were carried out on an MTS810 testing machine with a capacity of 500 kN and displacement control at a rate of 0.1 mm/min, according to the stipulations in ASTM C1609 [30]. The specimens were rotated normally 90° from the casting position to eliminate the eccentricity effect caused by the roughness of the surface. The f_{ftm} of the specimens was calculated as follows:

$$f_{\mathrm{ftm}} = \frac{Fl}{bh^2} \tag{2}$$

where f_{ftm} is the flexural strength (MPa), F is the maximum applied load shown by the testing machine (N), b, h is the average width and height of the specimen, respectively (mm), and l is the span length of the specimen (mm).

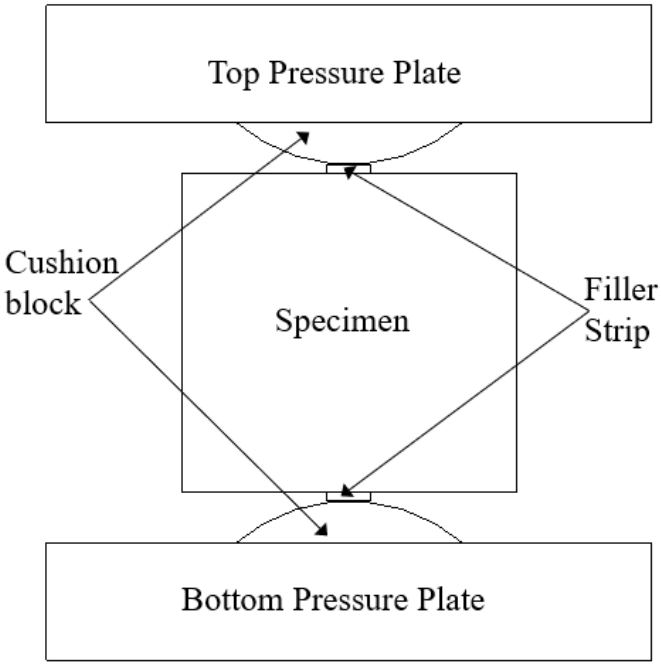


Figure 4. Test setup for splitting tensile strength.

The test results for each specimen group are the mean value of three specimens. The test results for f_{cu}, f_{ts}, and f_{tm} are listed in Table 5.

3. Test Results and Discussion

3.1. Compressive Strength

When the SF type is MF, the relations between f_{fcu} and SF V_f are as shown in Figure 5. Obviously, the f_{fcu} of SFNCAC is higher than that of SFRCAC when V_f increases from 0 to 2%. This is because RCA has more defects than NCA, and the matrix strength of RCAC is lower than that of NCAC with the same mixture proportions. This trend is evident in Table 4, which shows that the matrix strength of SFRCAC is lower than that of SFNCAC; many previous studies have reached the same conclusion [31,32]. However, when V_f increases from 0 to 2%, the f_{fcu} of SFNCAC and SFRCAC has a similar increasing trend. The curves of f_{fcu} for both SFNCAC and SFRCAC can be divided into three parts: in the first part ($0 < V_f \leq 0.5\%$), the compressive strength (f_{fcu}) for both of SFNCAC and SFRCAC increases gently; in the second part ($0.5\% < V_f \leq 1.5\%$), the f_{fcu} for both of SFNCAC and SFRCAC increases rapidly; in the third part ($1.5\% < V_f \leq 2\%$), the f_{fcu} of SFNCAC decreases slightly, while the f_{fcu} of SFRCAC still increases, with a small growth rate. From the analysis mentioned above, it can be concluded that the suitable dosage of SF is from 0.5% to 1.5% for the reinforcement effect on the f_{fcu} of SFNCAC and SFRCAC.

When $V_f = 1\%$, the relations of f_{fcu} with the SF type are as displayed in Figure 6. It can be concluded that the curves are close to straight lines and nearly parallel to one another, which indicates that the three types of SF (MF, BF, and SWF) have very similar effects on the f_{fcu} of SFNCAC and SFRCAC. This is because the compressive properties of SF-reinforced concrete are mainly controlled by the f_{fcu} of the concrete matrix [19]. The same kind of SF has the same reinforcing effect on concrete whether the concrete matrix is NCAC or RCAC. Of the three types of SF, MF has the best reinforcing effect on f_{fcu}; the other two kinds of SF have similar reinforcing effects. This may be because MF has a larger mean diameter than that of BF and SWF. For normal-strength concrete (40 MPa–60 MPa), the larger the mean diameter, the higher the f_{fcu}.

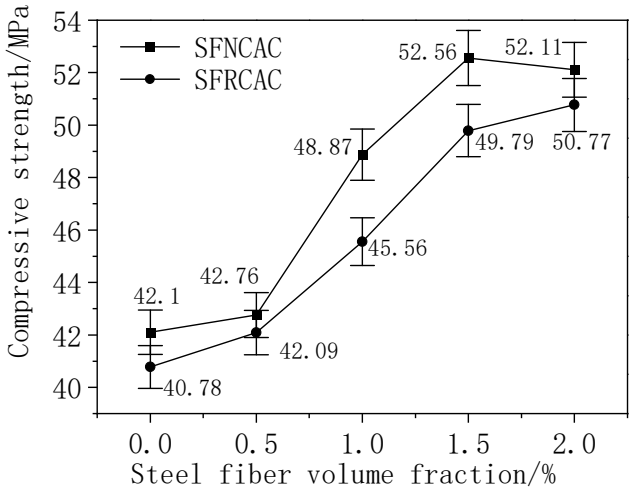


Figure 5. Relationships between compressive strength and steel fiber volume fraction.

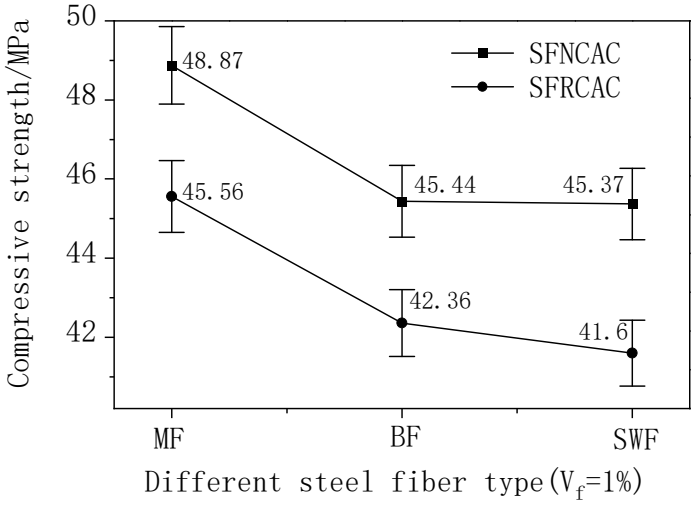


Figure 6. Relationships between compressive strength and steel fiber type.

3.2. Tensile Strength

When the SF type is MF, the relations between f_{fts} and SF V_f are as displayed in Figure 7. It can be concluded that the SF has same positive effect on the f_{fts} of both NCAC and RCAC. The curves of f_{fts} with SF V_f can be divided into three parts: in the first part ($0 < V_f \leq 0.5\%$), the increasing trends of f_{fts} for both NCAC and RCAC are very gentle; in the second part ($0.5\% < V_f \leq 1.5\%$), increases rapidly; f_{fts} is almost 5.5 MPa in the third part ($1.5\% < V_f \leq 2\%$). Therefore, when $V_f \leq 0.5\%$, SF only has a weak effect on f_{fts}; when $V_f > 1.5\%$, f_{fts} does not increase with the increase in V_f, but the f_{fts} of RCAC is very close to that of NCAC, and even surpasses that of NCAC when $V_f = 1.5\%$. This indicates that SF has a better reinforcing effect on the f_{fts} of RCAC than on that of NCAC when $V_f \geq 1.5\%$. On the whole, insufficient V_f cannot provide reinforcement to f_{fts}, while excessive V_f does not work well and wastes the material. The optimal dosage of SF is from 0.5% to 1.5% from the viewpoint of the reinforcement effect on the f_{fts} of NCAC and RCAC.

When $V_f = 1\%$, the relations between f_{fts} and the SF type are as displayed in Figure 8, based on the experimental data. It can be concluded that the curves for both NCAC and RCAC are nearly parallel to one another, which indicates that the three types of SF (MF, BF, and SWF) have similar effects on the f_{fts} of NCAC and RCAC. Of the three types of SF, BF has the best reinforcing effect on f_{fts}. As shown in Table 3, BF is almost twice as long as MF and SWF. Longer SF requires a stronger pullout force, and this may be the reason that

BF can provide the best reinforcing effect on f_{fts}. MF and SWF have similar lengths and provide similar reinforcing effects on f_{fts}.

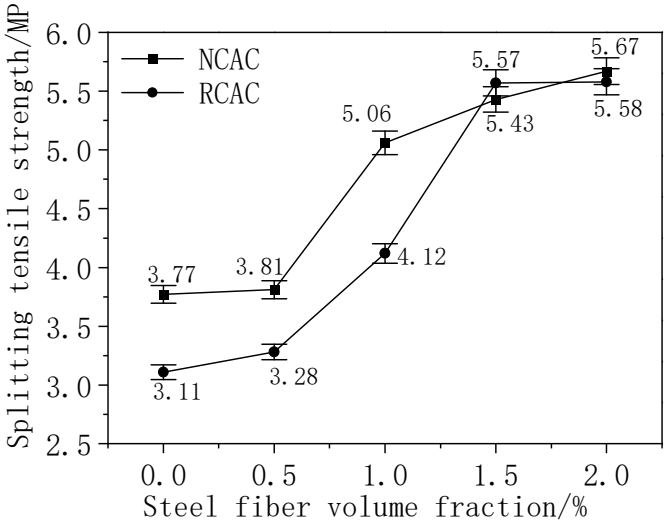


Figure 7. Relationships between splitting tensile strength and steel fiber volume fraction.

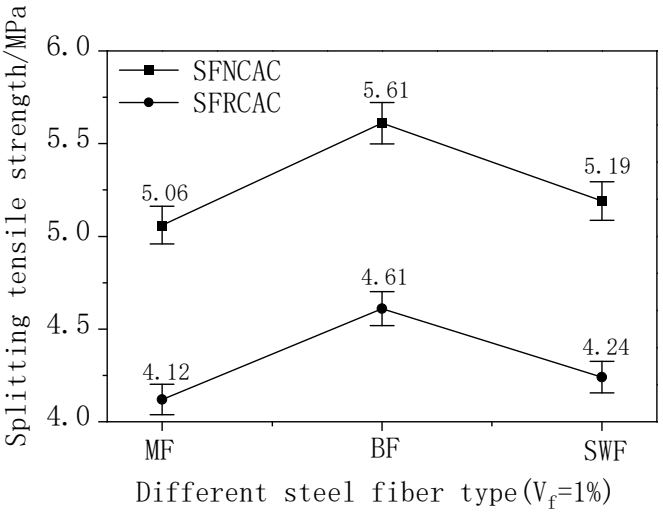


Figure 8. Relationships between splitting tensile strength and steel fiber type.

3.3. Flexural Strength

When the SF type is MF, the relations between f_{ftm} and SF V_f are as shown in Figure 9. Whether the concrete matrix is NCAC or RCAC, the f_{ftm} of NCAC and RCAC increases obviously with the increase in V_f. Although the f_{ftm} of NCAC is higher than that of RCAC, the lines showing the increases in the f_{ftm} of NCAC and RCAC are almost parallel to one another. This indicates that SF has the same reinforcing effect on the f_{ftm} of NCAC and RCAC. Unlike f_{fcu} and f_{fts}, which have optimal contents of SF (0.5–1.5%), when $V_f \leq 2\%$, the test results of f_{ftm} prove that the larger the V_f, the higher the f_{ftm}. Therefore, the upper limit of V_f for the f_{ftm} of NCAC and RCAC needs to be further studied.

When $V_f = 1\%$, the relations between f_{ftm} and the SF type are as displayed in Figure 10. It can be concluded that the curves for both NCAC and RCAC are parallel to one another, which indicates that the three types of SF (MF, BF, and SWF) have similar effects on the f_{ftm} of NCAC and RCAC. Of the three types of SF, BF has the best reinforcing effect on f_{ftm}, while SWF has a slightly better effect than MF. This may be because BF has the largest AR.

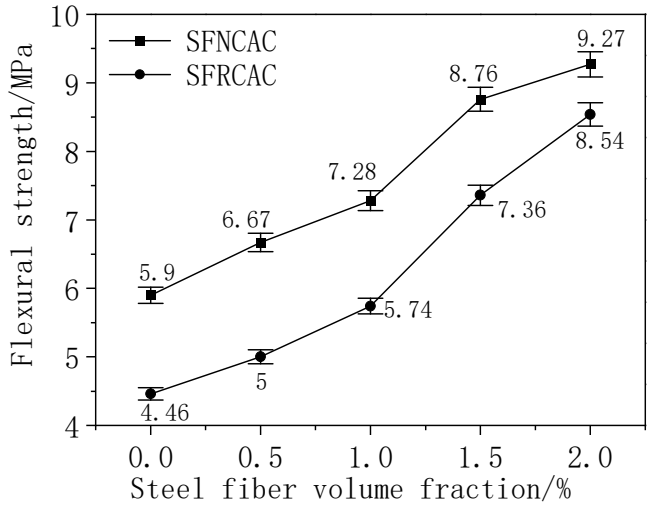


Figure 9. Relationships between flexural strength and steel fiber volume fraction.

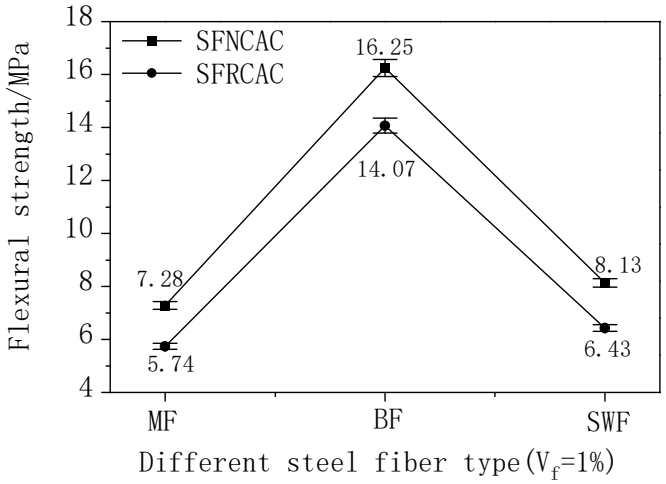


Figure 10. Relationships between flexural strength and steel fiber type.

3.4. Flexural Strength to Compressive Strength Ratio

The flexural strength–compressive strength ratio (F/C ratio) is often used to evaluate the toughness of cementitious composites [33]. When the SF type is MF, the relations between the F/C ratio and SF V_f are as shown in Figure 11. We can conclude that no matter whether the concrete matrix is NCAC or RCAC, the F/C ratio of NCAC and RCAC shows an increasing trend in general. Nevertheless, the F/C ratio of NCAC is consistently higher than that of RCAC regardless of the fiber doping, and it can also be seen that for the RCAC matrix, the most suitable SF doping is about 1%. Hence, it is interesting that the reinforcing effect of steel fiber on NCAC is more effective than on RCAC. This may result from the higher bonding strength between steel fiber and NCAC than between steel fiber and RCAC.

When V_f = 1%, the relations between the F/C ratio and SF type are as displayed in Figure 12. We can clearly see that the curve is similar to the f_{ftm} curve, and the lines showing the increases in the FC/ratio of NCAC and RCAC are almost parallel to one another. We can easily deduce that BF is more effective in improving the toughness of NCAC and RCAC.

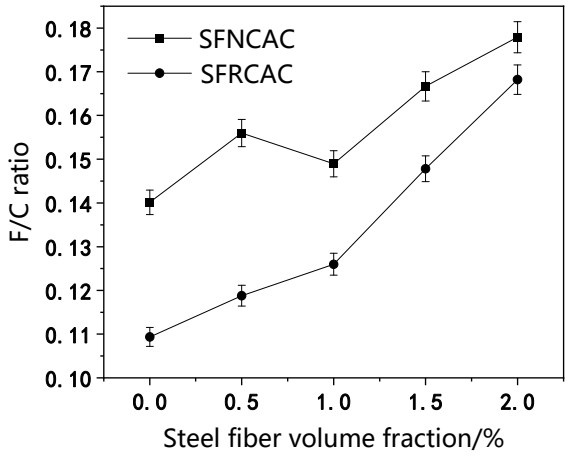


Figure 11. Relationships between flexural strength–compressive strength ratio and steel fiber volume fraction.

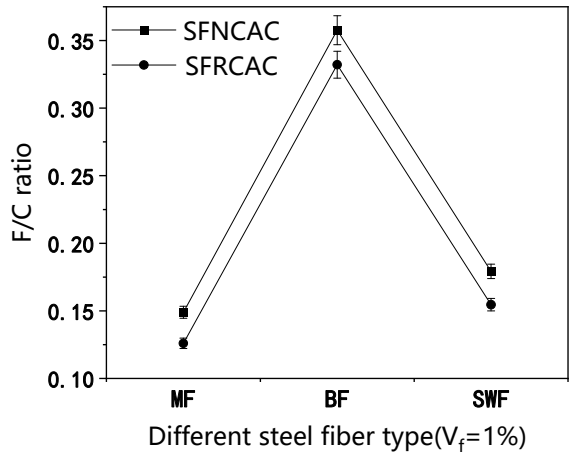


Figure 12. Relationships between flexural strength–compressive strength ratio and steel fiber type.

4. Reinforcing Effect of SF

4.1. Reinforcing Effect Evaluation

For the purpose of evaluating the effects of SF on the strength of NCAC and RCAC, the strength enhancement ratios (f_{fcu}/f_{cu}, f_{fts}/f_{ts}, f_{ftm}/f_{tm}), which are the ratios of the strength of SFRCAC to that of plain concrete with the same mixture proportions as SFRCAC without fibers, were calculated.

The relations of f_{fcu}/f_{cu}, f_{fts}/f_{ts} and f_{ftm}/f_{tm} with V_f are shown in Figure 13, according to the test results with the same type SF (MF). It can be concluded that for both NCAC and RCAC, the value of f_{fcu}/f_{cu} is smallest compared with that of f_{fts}/f_{ts} and f_{ftm}/f_{tm}. The value of f_{fcu}/f_{cu} for both NCAC and RCAC with V_f = 1% reached the maximum of 1.18, and it was below 1.1 for the other case, which is far below the values of f_{fts}/f_{ts} and f_{ftm}/f_{tm}. These results are consistent with those reported in the literature, indicating that the adding SF to concrete can increase the f_{ts} by a factor of 1.5–2, with a slight increase in f_{cu} (up to 10–25%) [34]. Only when V_f = 0.5% is the value of f_{ftm}/f_{tm} for NCAC larger than 1.1, which indicates that when $V_f \leq 0.5\%$, steel fiber has a slight reinforcing effect on the f_{fts} and f_{ftm} of NCAC, except for the f_{ftm} of SFNCAC. The values of both f_{fts}/f_{ts} and f_{ftm}/f_{tm} increase rapidly when $V_f \geq 1\%$; moreover, the value of f_{fts}/f_{ts} is larger than that of f_{ftm}/f_{tm}. When V_f = 2%, the value of f_{fts}/f_{ts} for SFNCAC reaches the maximum of 1.76, while it is 1.68 for SFRCAC. The value of f_{ftm}/f_{tm} for SFNCAC is very close to that for SFRCAC, especially when V_f = 1.5%, with the same value of 1.33.

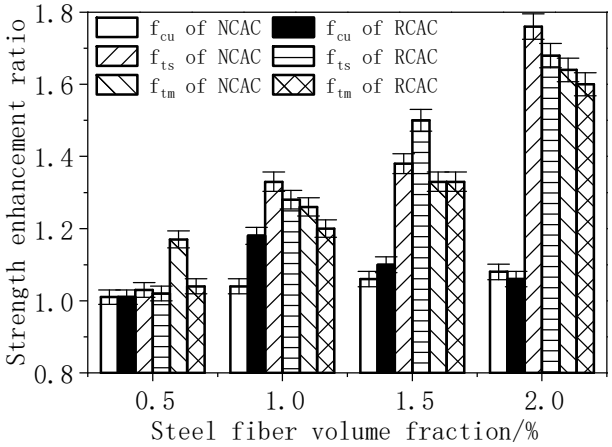


Figure 13. Relationships between strength enhancement ratio and steel fiber volume fraction.

For the purpose of evaluating the reinforcing effect of SF type on f_{fcu}, f_{fts}, and f_{ftm}, the values of f_{fcu}/f_{cu}, f_{fts}/f_{ts}, and f_{ftm}/f_{tm} reinforced by MF, BF, and SF (V_f = 1%) were also calculated. The relations of f_{fcu}/f_{cu}, f_{fts}/f_{ts}, and f_{ftm}/f_{tm} with SF type are given in Figure 14. The values of f_{fcu}/f_{cu} for the three types of SF are less than 1.1, and they are all lower than those of f_{fts}/f_{ts} and f_{ftm}/f_{tm}. This indicates that the reinforcing effect of these three types of SF on f_{fcu} is less than that on f_{fts} and f_{ftm}. MF and SWF have similar reinforcing effects on f_{fcu}, f_{fts}, and f_{ftm}; the values of f_{fts}/f_{ts} and f_{ftm}/f_{tm} for SFNCAC and SFRCAC are around 1.3 and 1.4, respectively. The values of f_{fts}/f_{ts} for SFNCAC and SFRCAC with BF are 1.47 and 1.43, respectively, which are slightly higher than those with MF and SWF. However, the values of f_{fts}/f_{ts} for SFNCAC and SFRCAC with BF are 2.81 and 2.94, respectively, which are much higher than those with MF and SWF. This may be due to the fact that the AR values of MF and SF are very close, while the AR of BF is almost twice that of the other two types of SF. When V_f is determined, the values of f_{fts}/f_{ts} and f_{ftm}/f_{tm} increase significantly with the increase in the SF aspect ratio (AR).

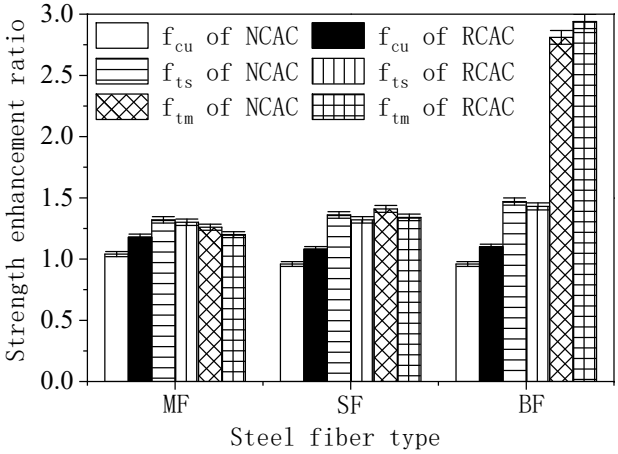


Figure 14. Relationships between strength enhancement ratio and steel fiber type.

4.2. Reinforcing Effect Calculation

Based on the above analysis, SF has similar reinforcing effects on NCAC and RCAC. The reinforcing effect of SF on f_{fcu} is not as obvious as on f_{fts} and f_{ftm}. The values of f_{fts}/f_{ts} and f_{ftm}/f_{tm} are related to the V_f and aspect ratio. These two factors can be reflected by the SF characteristic coefficient (λ_f), $\lambda_f = V_f l_f/d_f$. The relations between f_{fts}/f_{ts}, f_{ftm}/f_{tm}, and λ_f, according to the experimental data in this paper and the previous literature [35], are shown in Figure 15.

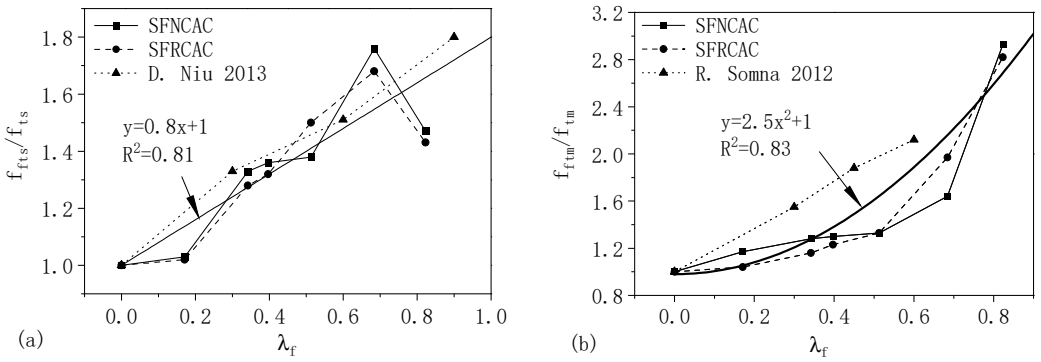


Figure 15. Relationships between strength enhancement ratio and characteristic coefficient of steel fiber (**a**) f_{ts} [34]; (**b**) f_{tm} [36].

As shown in Figure 15a, the change in f_{fts}/f_{ts} for SFNCAC and SFRCAC follows the same trend, where both increase with the increase in λ_f. Except for two points, where the steel fiber is BF and V_f = 1%, the value of f_{fts}/f_{ts} decreases obviously with the increase in λ_f. As shown in Table 3, the length of BF is 62 mm, and its AR is 82.3; both the length and AR of BF are much higher than those of other two types of SF. The length of the specimens for the splitting tensile strength tests was 150 mm; therefore, the distribution uniformity of SF in the specimens may decrease if the SF is too long. This may lead to the content of SF being too small in partial sites, the internal defects of SFNCAC and SFRCAC increase, and the stress easily concentrates under the action of loading. With the increase in λ_f, the value of f_{fts}/f_{ts} does not increase, but rather decreases. Therefore, the long SF is not suitable for the small specimens, as the reinforcing effect could be weakened due to the inhomogeneous distribution of SF. As shown in Figure 15a, the reinforcing ratio of f_{ts} is approximately linear with the increase in λ_f. According to the test data of this paper and the literature [34], a linear regression equation between f_{fts}/f_{ts} and λ_f is put forward as follows:

$$f_{fts}/f_{ts} = 0.8\lambda_f + 1 \left(R^2 = 0.81\right) \quad (3)$$

where f_{fts} is the splitting tensile strength of SFRCAC, f_{ts} is the splitting tensile strength of RCAC with the same mix proportions as the SFRCAC, and λ_f is the characteristic parameter of steel fiber.

As shown in Figure 15b, the values of f_{ftm}/f_{tm} for both SFNCAC and SFRCAC increase with the increase in λ_f. When λ_f is less than 0.5, the value of f_{ftm}/f_{tm} increases slowly; however, it increases rapidly when λ_f is above 0.5. The relationship between f_{ftm}/f_{tm} and λ_f is quadratic. Based on regression analysis of the experimental data from this paper and the literature [36], a regression equation between f_{ftm}/f_{tm} and λ_f is proposed as follows:

$$f_{ftm}/f_{tm} = 2.5 \times \lambda_f^2 + 1 \left(R^2 = 0.83\right) \quad (4)$$

where f_{ftm} is the flexural strength of SFRCAC, while f_{tm} is the flexural strength of RCAC with the same mix proportions as the SFRCAC.

For the required f_{fts} or f_{ftm} of SFRCAC, the λ_f can be determined using Equation (3) when f_{ts} is known, or using Equation (4) when f_{tm} is known. The SF type and AR can be chosen according to the engineering requirements. Finally, the V_f can be calculated.

5. Value Engineering Analysis

Value engineering analysis is a quantitative method of analyzing the value of a product in terms of the features that it possesses compared to the cost that it requires. Value (V) = Function (F)/Cost (C). The value engineering analysis method was used to perform a cost analysis of steel-fiber-reinforced recycled aggregate concrete.

According to the experimental results, it can be seen that the mechanical properties of concrete can be significantly improved when SF is added. Among them, SFNCAC had the highest strength, while the mechanical properties of SFRCAC were lower than those of SFNCAC but significantly higher than those of ordinary concrete and recycled aggregate concrete. However, the cost of SFNCAC is much higher than that of SFRCAC. Among them, the cost of SFNCAC is the highest, at CNY 725.75, while the cost of SFRCAC is similar to or even lower than that of NCAC, at CNY 468.66.

According to the value engineering analysis method, the value of the samples was analyzed and compared, as shown in Table 6. It can be inferred that although RCAC has the best cost performance, its mechanical properties are the worst, which makes it difficult to apply in practical engineering. Compared with SFNCAC, SFRCAC has lower cost and similar mechanical properties, which means that it has better cost performance.

Table 6. Value engineering analysis.

Specimen Designation	NCAC	RCAC	SFNCAC	SFRCAC
f_{cu}/MPa	48.29	48.07	52.11	50.77
f_{ts}/MPa	3.23	3.32	5.67	5.58
f_{tm}/MPa	5.65	5.34	9.27	8.54
Strength evaluation	19.06	18.91	22.35	21.63
Total cost	491.75	234.66	725.75	468.66
Value	0.04	0.08	0.03	0.05

Note: Strength evaluation represents only the evaluation of the strength of the specimen and has no practical significance.

6. Conclusions

The reinforcing effects of SF on the f_{fcu}, f_{fts}, and f_{ftm} of SFNCAC and SFRCAC were studied through experiments. Based on the experimental results and analysis, the following conclusions can be drawn:

1. Steel fiber has the same reinforcing effect on NCAC and RCAC. For RCAC, the suitable content range of SF is from 0.5% to 1.5% of V_f in terms of the reinforcement effects on f_{fcu} and f_{fts}. When $V_f \leq 2\%$, the larger the V_f, the higher the f_{ftm}. The upper limit of V_f for f_{ftm} needs to be further studied.
2. The reinforcing effect of SF on the strength of SFRCAC is related to the strength of the RCAC matrix. When all other conditions are equal, the SF with the larger diameter has the better reinforcing effect on the f_{fcu} of RCAC; the steel fiber with the higher AR has the better reinforcing effect on the f_{fts} and f_{ftm} of RCAC.
3. Among the three types of steel fibers, MF and SF have similar reinforcing effects on f_{fcu}, f_{fts}, and f_{ftm}, However, the f_{fts}/f_{ts} values of SFNCAC and SFRCAC with BF are much higher than those with MF and SF because of the larger aspect ratio of the former.
4. According to the value engineering analysis method, it can be inferred that although RCAC has the best cost performance, its mechanical properties are the worst, which makes it difficult to apply in practical engineering. Compared with SFNCAC, SFRCAC has lower cost and similar mechanical properties, which means that it has better cost performance.
5. The positive reinforcing effect of SF on the f_{fts} and f_{ftm} of RCAC is much better than that on f_{fcu}. A linear regression equation between f_{fts}/f_{ts} and λ_f, and a quadratic equation between f_{ftm}/f_{tm} and λ_f of SFRCAC, were put forward. The content of steel fiber can be calculated by Equation (3) or Equation (4) when the required f_{ts} or f_{tm} of RCAC is given, respectively.

Author Contributions: Conceptualization, Y.W.; Methodology, L.L.; Formal analysis, L.Z.; Resources, P.Y.; Writing—original draft, P.Y., Z.M., L.Z., Y.W., Q.F. and L.L.; Writing—review & editing, P.Y., Z.M., L.Z., Y.W., Q.F. and L.L.; Supervision, Z.M.; Project administration, Q.F. All authors have read and agreed to the published version of the manuscript.

Funding: This work was part of a key project financially supported by the National Natural Science Foundation of China (52108207, 51808509, 52109168), Natural Science Foundation of Henan (212300410106), Henan Province Key Science and Technology Attack Plan Project (212102310281), Young Backbone Teachers Project of Henan University of Urban Construction (YCJQNGGJS202002), Academic and Technical Leaders Project of Henan University of Urban Construction (YCJXSJSDTR202201), and Innovation and Entrepreneurship Training Program for University Students (202211765031).

Data Availability Statement: No new data was created.

Conflicts of Interest: The authors declare no conflict of interest.

References

1. Raman, J.V.M.; Ramasamy, V. Various treatment techniques involved to enhance the recycled coarse aggregate in concrete: A review. *Mater. Today Proc.* **2021**, *45*, 6356–6363. [CrossRef]
2. Ma, Z.; Shen, J.; Wang, C.; Wu, H. Characterization of sustainable mortar containing high-quality recycled manufactured sand crushed from recycled coarse aggregate. *Cem. Concr. Compos.* **2022**, *132*, 104629. [CrossRef]
3. Liu, H.; Liu, C.; Wu, Y.; Bai, G.; He, C.; Zhang, R.; Wang, Y. Hardened properties of 3D printed concrete with recycled coarse aggregate. *Cem. Concr. Res.* **2022**, *159*, 106868. [CrossRef]
4. Bao, J.; Li, S.; Zhang, P.; Ding, X.; Xue, S.; Cui, Y.; Zhao, T. Influence of the incorporation of recycled coarse aggregate on water absorption and chloride penetration into concrete. *Constr. Build Mater.* **2020**, *239*, 117845. [CrossRef]
5. Salesa, N.; Pérez-Benedicto, J.A.; Colorado-Aranguren, D.; López-Julián, P.L.; Esteban, L.M.; Sanz-Baldúz, L.J.; Sáez-Hostaled, J.L.; Ramis, J.; Olivares, D. Physico-mechanical properties of multi-recycled concrete from precast concrete industry. *J. Clean. Prod.* **2017**, *141*, 248–255. [CrossRef]
6. Shi, C.; Li, Y.; Zhang, J.; Li, W.; Chong, L.; Xie, Z. Performance enhancement of recycled concrete aggregate—A review. *J. Clean. Prod.* **2016**, *112*, 466–472. [CrossRef]
7. Kubissa, J.; Koper, M.; Koper, W.O.; Kubissa, W. Koper. Water Demand of Concrete Recycled Aggregates. *Procedia Eng.* **2015**, *108*, 63–71. [CrossRef]
8. Hamad, B.S.; Dawi, A.H. Sustainable normal and high strength recycled aggregate concretes using crushed tested cylinders as coarse aggregates. *Case Stud. Constr. Mater.* **2017**, *7*, 228–239. [CrossRef]
9. Bravo, M.; de Brito, J.; Evangelista, L.; Pacheco, J. Superplasticizer's efficiency on the mechanical properties of recycled aggregates concrete: Influence of recycled aggregates composition and incorporation ratio. *Constr. Build. Mater.* **2017**, *153*, 129–138. [CrossRef]
10. He, Z.; Zhang, J. Strength characteristics and failure criterion of plain recycled aggregate concrete under triaxial stress states. *Constr. Build. Mater.* **2014**, *54*, 354–362. [CrossRef]
11. Omary, S.; Ghorbel, E. Wardeh. Relationships between recycled concrete aggregates characteristics and recycled aggregates concretes properties. *Constr. Build. Mater.* **2016**, *108*, 163–174. [CrossRef]
12. Khodair, Y.; Bommareddy, B. Self-consolidating concrete using recycled concrete aggregate and high volume of fly ash, and slag. *Constr. Build. Mater.* **2017**, *153*, 307–316. [CrossRef]
13. Ding, T.; Xiao, J.; Tam, V.W.Y. A closed-loop life cycle assessment of recycled aggregate concrete utilization in China. *Waste Manag.* **2016**, *56*, 367–375. [CrossRef] [PubMed]
14. Xiao, J.; Li, W.; Fan, Y.; Huang, X. An overview of study on recycled aggregate concrete in China (1996–2011). *Constr. Build. Mater.* **2012**, *31*, 364–383. [CrossRef]
15. Afroughsabet, V.; Biolzi, L.; Ozbakkaloglu, T. Influence of double hooked-end steel fibers and slag on mechanical and durability properties of high performance recycled aggregate concrete. *Compos. Struct.* **2017**, *181*, 273–284.
16. Carneiro, J.A.; Lima, P.R.L.; Leite, M.N.B.; Filho, R.D.T. Compressive stress–strain behavior of steel fiber reinforced-recycled aggregate concrete. *Cem. Concr. Compos.* **2014**, *46*, 65–72. [CrossRef]
17. Gao, D.; Zhang, L.; Nokken, M. Mechanical behavior of recycled coarse aggregate concrete reinforced with steel fibers under direct shear. *Cem. Concr. Compos.* **2017**, *79*, 1–8. [CrossRef]
18. Li, L.; Yan, C.; Zhang, N.; Farooqi, M.U.; Xu, S.; Deifalla, A.F. Flexural fracture parameters of polypropylene fiber reinforced geopolymer. *J. Mater. Res. Technol.* **2023**, *24*, 1839–1855. [CrossRef]
19. Li, L.; Qin, Y.; Cao, M.; Guan, J.; Xie, C. Bending performance and calculation of reinforced beam with hybrid fiber and $CaCO_3$ whisker. *Comput. Concr.* **2023**, *31*, 197–206.
20. Gao, D.; Zhu, W.; Fang, D.; Tang, J.; Zhu, H. Shear behavior analysis and capacity prediction for the steel fiber reinforced concrete beam with recycled fine aggregate and recycled coarse aggregate. *Structures* **2022**, *37*, 44–55. [CrossRef]
21. Li, L.; Ma, Z.; Ming, X. Multiscale ab-initio modeling and experiment of nano-$CaCO_3$ and fiber synergy on toughening low-carbon geopolymer composites. *Mater. Des.* **2023**, *233*, 112280. [CrossRef]

22. Jang, S.; Yun, H. Combined effects of steel fiber and coarse aggregate size on the compressive and flexural toughness of high-strength concrete. *Compos. Struct.* **2018**, *185*, 203–211. [CrossRef]
23. *GB/175-2007*; Common Portland Cement. China Standards Press: Beijing, China, 2007.
24. *ASTM C33-13*; Standard Specification for Concrete Aggregates. ASTM: West Conshohocken, PA, USA, 2013.
25. *GB/T 25177*; Recycled Coarse Aggregate for Concrete. China Standards Press: Beijing, China, 2010.
26. *GB/T 14685*; Pebble and Crushed Stone for Construction. China Standards Press: Beijing, China, 2011.
27. *JGJ/T 221-2010*; Technical Specification for Application of Fiber Reinforced Concrete. China National Standardization Administration: Beijing, China, 2010.
28. Gao, D.; Zhao, J.; Zhu, H. *Design and Application of Steel Fiber Concrete*; China Construction Industry Press: Beijing, China, 2002.
29. *GB/T50081*; Standard for Test Method of Mechanical Properties on Ordinary Concrete. China Architecture & Building Press: Beijing, China, 2002.
30. *ASTM C1609*; Standard Test Method for Flexural Performance of Fiber-Reinforced Concrete (Using Beam with Third-Point Loading). ASTM International: West Conshohocken, PA, USA, 2012.
31. Mukharjee, B.B.; Barai, S.V. Influence of incorporation of nano-silica and recycled aggregates on compressive strength and microstructure of concrete. *Constr. Build. Mater.* **2014**, *71*, 570–578. [CrossRef]
32. Silva, R.V.; de Brito, J.; Dhir, R.K. Establishing a relationship between modulus of elasticity and compressive strength of recycled aggregate concrete. *J. Clean. Prod.* **2016**, *112*, 2171–2186.
33. Cao, M.; Zhang, C.; Li, Y.; Wei, J. Using Calcium Carbonate Whisker in Hybrid Fiber-Reinforced Cementitious Composites. *J. Mater. Civ. Eng.* **2015**, *27*, 4014139. [CrossRef]
34. Niu, D.; Jiang, L.; Bai, M.; Miao, Y. Study of the performance of steel fiber reinforced concrete to water and salt freezing condition. *Mater. Des.* **2013**, *44*, 267–273. [CrossRef]
35. Kim, H.; Kim, G.; Gucunski, N.; Nam, J.; Jeon, J. Assessment of flexural toughness and impact resistance of bundle-type polyamide fiber-reinforced concrete. *Compos. Part B Eng.* **2015**, *78*, 431–446. [CrossRef]
36. Somna, R.; Jaturapitakkul, C.; Chalee, W.; Rattanachu, P. Effect of the Water to Binder Ratio and Ground Fly Ash on Properties of Recycled Aggregate Concrete. *J. Mater. Civ. Eng.* **2012**, *24*, 16–22. [CrossRef]

Disclaimer/Publisher's Note: The statements, opinions and data contained in all publications are solely those of the individual author(s) and contributor(s) and not of MDPI and/or the editor(s). MDPI and/or the editor(s) disclaim responsibility for any injury to people or property resulting from any ideas, methods, instructions or products referred to in the content.